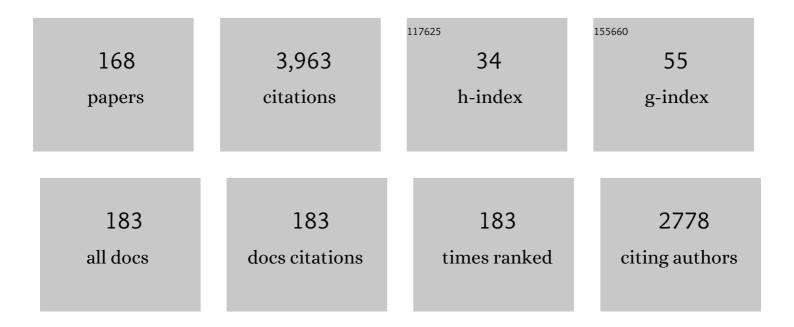
List of Publications by Year in descending order

Source: https://exaly.com/author-pdf/5029310/publications.pdf Version: 2024-02-01



#	Article	IF	CITATIONS
1	Hydraulic Fracturing and Seismicity in the Western Canada Sedimentary Basin. Seismological Research Letters, 2016, 87, 631-647.	1.9	329
2	Self-organization in leaky threshold systems: The influence of near-mean field dynamics and its implications for earthquakes, neurobiology, and forecasting. Proceedings of the National Academy of Sciences of the United States of America, 2002, 99, 2514-2521.	7.1	161
3	Surface uplift and time-dependent seismic hazard due to fluid injection in eastern Texas. Science, 2016, 353, 1416-1419.	12.6	127
4	The 2011 Lorca earthquake slip distribution controlled by groundwater crustal unloading. Nature Geoscience, 2012, 5, 821-825.	12.9	123
5	Mean-field threshold systems and phase dynamics: An application to earthquake fault systems. Europhysics Letters, 2002, 60, 481-488.	2.0	115
6	Linear pattern dynamics in nonlinear threshold systems. Physical Review E, 2000, 61, 2418-2431.	2.1	99
7	Rapidly accelerating subsidence in the Greater Vancouver region from two decades of ERS-ENVISAT-RADARSAT-2 DInSAR measurements. Remote Sensing of Environment, 2014, 143, 180-191.	11.0	98
8	Space-Time Clustering and Correlations of Major Earthquakes. Physical Review Letters, 2006, 97, 238501.	7.8	89
9	Pattern Dynamics and Forecast Methods in Seismically Active Regions. Pure and Applied Geophysics, 2002, 159, 2429-2467.	1.9	85
10	Analytical Optimization of a DInSAR and GPS Dataset for Derivation of Three-Dimensional Surface Motion. IEEE Geoscience and Remote Sensing Letters, 2006, 3, 107-111.	3.1	85
11	A RELM Earthquake Forecast Based on Pattern Informatics. Seismological Research Letters, 2007, 78, 87-93.	1.9	85
12	Magma storage and migration associated with the 2011–2012 El Hierro eruption: Implications for crustal magmatic systems at oceanic island volcanoes. Journal of Geophysical Research: Solid Earth, 2013, 118, 4361-4377.	3.4	83
13	Seismicity-based earthquake forecasting techniques: Ten years of progress. Tectonophysics, 2012, 522-523, 89-121.	2.2	79
14	Application of DInSAR-GPS Optimization for Derivation of Fine-Scale Surface Motion Maps of Southern California. IEEE Transactions on Geoscience and Remote Sensing, 2007, 45, 512-521.	6.3	76
15	A simultaneous inversion for deformation rates and topographic errors of DInSAR data utilizing linear least square inversion technique. Computers and Geosciences, 2011, 37, 1083-1091.	4.2	73
16	The 1999 Chi-Chi, Taiwan, earthquake as a typical example of seismic activation and quiescence. Geophysical Research Letters, 2005, 32, n/a-n/a.	4.0	65
17	Virtual California: Fault Model, Frictional Parameters, Applications. Pure and Applied Geophysics, 2006, 163, 1819-1846.	1.9	60
18	Local quaternion Fourier transform and color image texture analysis. Signal Processing, 2010, 90, 1825-1835.	3.7	52

#	Article	IF	CITATIONS
19	Shallow flank deformation at Cumbre Vieja volcano (Canary Islands): Implications on the stability of steep-sided volcano flanks at oceanic islands. Earth and Planetary Science Letters, 2010, 297, 545-557.	4.4	51
20	Modification of the pattern informatics method for forecasting large earthquake events using complex eigenfactors. Tectonophysics, 2006, 413, 87-91.	2.2	48
21	Ergodicity in natural earthquake fault networks. Physical Review E, 2007, 75, 066107.	2.1	48
22	A simulation-based approach to forecasting the next great San Francisco earthquake. Proceedings of the United States of America, 2005, 102, 15363-15367.	7.1	46
23	Systematic Procedural and Sensitivity Analysis of the Pattern Informatics Method for Forecasting Large (M > 5) Earthquake Events in Southern California. Pure and Applied Geophysics, 2006, 163, 2433-2454.	1.9	43
24	Modeling the two- and three-dimensional displacement field in Lorca, Spain, subsidence and the global implications. Scientific Reports, 2018, 8, 14782.	3.3	42
25	Structure of fluctuations near mean-field critical points and spinodals and its implication for physical processes. Physical Review E, 2007, 75, 031114.	2.1	40
26	Nonlinear Network Dynamics on Earthquake Fault Systems. Physical Review Letters, 2001, 87, 148501.	7.8	39
27	Detection of displacements on Tenerife Island, Canaries, using radar interferometry. Geophysical Journal International, 2004, 160, 33-45.	2.4	38
28	Probabilities for large events in driven threshold systems. Physical Review E, 2012, 86, 021106.	2.1	38
29	What drives large-scale glacier detachments? Insights from Flat Creek glacier, St. Elias Mountains, Alaska. Geology, 2020, 48, 703-707.	4.4	38
30	Results of the Regional Earthquake Likelihood Models (RELM) test of earthquake forecasts in California. Proceedings of the National Academy of Sciences of the United States of America, 2011, 108, 16533-16538.	7.1	37
31	Spatiotemporal analysis and interpretation of 1993–2013 ground deformation at Campi Flegrei, Italy, observed by advanced DInSAR. Geophysical Research Letters, 2014, 41, 6101-6108.	4.0	37
32	Inflation or deflation? New results for Mayon Volcano applying elastic-gravitational modeling. Geophysical Research Letters, 2001, 28, 2349-2352.	4.0	36
33	Using earthquake intensities to forecast earthquake occurrence times. Nonlinear Processes in Geophysics, 2006, 13, 585-593.	1.3	36
34	Removal of systematic seasonal atmospheric signal from interferometric synthetic aperture radar ground deformation time series. Geophysical Research Letters, 2014, 41, 6123-6130.	4.0	36
35	Spatiotemporal variations in vertical gravity gradients at the Campi Flegrei caldera (Italy): a case for source multiplicity during unrest?. Geophysical Journal International, 2006, 167, 1089-1096.	2.4	35
36	Nyamulagira's magma plumbing system inferred from 15 years of InSAR. Geological Society Special Publication, 2013, 380, 39-65.	1.3	35

#	Article	IF	CITATIONS
37	Modeling of fast ground subsidence observed in southern Saskatchewan (Canada) during 2008–2011. Natural Hazards and Earth System Sciences, 2014, 14, 247-257.	3.6	35
38	Quantitative Analysis of Seismicity in Iran. Pure and Applied Geophysics, 2017, 174, 793-833.	1.9	35
39	Earthquake precursors: activation or quiescence?. Geophysical Journal International, 2011, 187, 225-236.	2.4	34
40	Ground deformation in the Taupo Volcanic Zone, New Zealand, observed by ALOS PALSAR interferometry. Geophysical Journal International, 2011, 187, 147-160.	2.4	32
41	Application of DInSAR-GPS optimization for derivation of three-dimensional surface motion of the southern California region along the San Andreas fault. Computers and Geosciences, 2008, 34, 503-514.	4.2	31
42	Detailed multidisciplinary monitoring reveals pre- and co-eruptive signals at Nyamulagira volcano (North Kivu, Democratic Republic of Congo). Bulletin of Volcanology, 2014, 76, 1.	3.0	31
43	Detection of volcanic unrest onset in La Palma, Canary Islands, evolution and implications. Scientific Reports, 2021, 11, 2540.	3.3	31
44	Dynamics of seismicity patterns in systems of earthquake faults. Geophysical Monograph Series, 2000, , 127-146.	0.1	28
45	GEM Plate Boundary Simulations for the Plate Boundary Observatory: A Program for Understanding the Physics of Earthquakes on Complex Fault Networks via Observations, Theory and Numerical Simulation. Pure and Applied Geophysics, 2002, 159, 2357-2381.	1.9	28
46	Viscoelastic displacement and gravity changes due to point magmatic intrusions in a gravitational layered solid earth. Geophysical Journal International, 2001, 146, 155-170.	2.4	27
47	Volcanic source inversion using a genetic algorithm and an elastic-gravitational layered earth model for magmatic intrusions. Computers and Geosciences, 2004, 30, 985-1001.	4.2	27
48	Joint interpretation of displacement and gravity data in volcanic areas. A test example: Long Valley Caldera, California. Geophysical Research Letters, 2001, 28, 1063-1066.	4.0	26
49	Multidimensional Small Baseline Subset (MSBAS) for volcano monitoring in two dimensions: Opportunities and challenges. Case study Piton de la Fournaise volcano. Journal of Volcanology and Geothermal Research, 2017, 344, 121-138.	2.1	26
50	From Tornadoes to Earthquakes: Forecast Verification for Binary Events Applied to the 1999 Chi-Chi, Taiwan,Earthquake. Terrestrial, Atmospheric and Oceanic Sciences, 2006, 17, 503.	0.6	26
51	New Approach to Gutenberg-Richter Scaling. Physical Review Letters, 2011, 106, 108501.	7.8	23
52	Polarization Phase Difference Analysis for Selection of Persistent Scatterers in SAR Interferometry. IEEE Geoscience and Remote Sensing Letters, 2011, 8, 331-335.	3.1	22
53	Analysis of complex networks associated to seismic clusters near the Itoiz reservoir dam. European Physical Journal: Special Topics, 2009, 174, 181-195.	2.6	21
54	Forecasting the Locations of Future Large Earthquakes: An Analysis and Verification. Pure and Applied Geophysics, 2010, 167, 743-749.	1.9	21

#	Article	IF	CITATIONS
55	Spatio-temporal analysis of ground deformation occurring near Rice Lake, Saskatchewan, and observed by Radarsat-2 DInSAR during 2008–2011. Canadian Journal of Remote Sensing, 2013, 39, 27-33.	2.4	20
56	New Results at Mayon, Philippines, from a Joint Inversion of Gravity and Deformation Measurements. Pure and Applied Geophysics, 2004, 161, 1433-1452.	1.9	19
57	Analysis of GPS Measurements in Eastern Canada Using Principal Component Analysis. Pure and Applied Geophysics, 2012, 169, 1483-1506.	1.9	19
58	Record-breaking avalanches in driven threshold systems. Physical Review E, 2013, 87, 052811.	2.1	19
59	Real-Time Earthquake Intensity Estimation Using Streaming Data Analysis of Social and Physical Sensors. Pure and Applied Geophysics, 2017, 174, 2331-2349.	1.9	19
60	Using Eigenpattern Analysis to Constrain Seasonal Signals in Southern California. Pure and Applied Geophysics, 2004, 161, 1991.	1.9	18
61	Premonitory seismicity changes prior to the Parkfield and Coalinga earthquakes in southern California. Tectonophysics, 2006, 413, 77-86.	2.2	18
62	The trinion Fourier transform of color images. Signal Processing, 2011, 91, 1887-1900.	3.7	18
63	Testing the persistence in earthquake catalogs: The Iberian Peninsula. Europhysics Letters, 2006, 73, 171-177.	2.0	17
64	On the interpretation of vertical gravity gradients produced by magmatic intrusions. Journal of Geodynamics, 2005, 39, 475-492.	1.6	16
65	Gravity changes from a stress evolution earthquake simulation of California. Journal of Geophysical Research, 2006, 111, .	3.3	16
66	Time Localised Band Filtering Using Modified S-Transform. , 2009, , .		16
67	Ground deformation occurring in the city of Auckland, New Zealand, and observed by Envisat interferometric synthetic aperture radar during 2003–2007. Journal of Geophysical Research, 2010, 115,	3.3	16
68	Hazard Implications of the 2016 Mw 5.0 Cushing, OK Earthquake from a Joint Analysis of Damage and InSAR Data. Remote Sensing, 2018, 10, 1715.	4.0	16
69	SAR-derived flow velocity and its link to glacier surface elevation change and mass balance. Remote Sensing of Environment, 2021, 258, 112343.	11.0	16
70	Critical point theory of earthquakes: Observation of correlated and cooperative behavior on earthquake fault systems. Geophysical Research Letters, 2006, 33, n/a-n/a.	4.0	15
71	Time Evolution of Deformation Using Time Series of Differential Interferograms: Application to La Palma Island (Canary Islands). Pure and Applied Geophysics, 2008, 165, 1531-1554.	1.9	15
72	Geodetic and Structural Research in La Palma, Canary Islands, Spain: 1992–2007 Results. Pure and Applied Geophysics, 2009, 166, 1461-1484.	1.9	15

#	Article	IF	CITATIONS
73	Ergodicity and Earthquake Catalogs: Forecast Testing and Resulting Implications. Pure and Applied Geophysics, 2010, 167, 763-782.	1.9	15
74	A tri-stage cluster identification model for accurate analysis of seismic catalogs. Nonlinear Processes in Geophysics, 2013, 20, 143-162.	1.3	15
75	The Predictive Relationship between Earthquake Intensity and Tweets Rate for Realâ€Time Groundâ€Motion Estimation. Seismological Research Letters, 2017, 88, 840-850.	1.9	14
76	Pattern informatics approach to earthquake forecasting in 3D. Concurrency Computation Practice and Experience, 2010, 22, 1569-1592.	2.2	13
77	A simple metric to quantify seismicity clustering. Nonlinear Processes in Geophysics, 2010, 17, 293-302.	1.3	13
78	Testing the Pattern Informatics index on synthetic seismicity catalogs based on the Non-Critical PAST. Tectonophysics, 2010, 483, 255-268.	2.2	12
79	Fast subsidence in downtown of Seattle observed with satellite radar. Remote Sensing Applications: Society and Environment, 2016, 4, 179-187.	1.5	12
80	Earthquake forecasting and its verification in northeast India. Geomatics, Natural Hazards and Risk, 2016, 7, 194-214.	4.3	12
81	Principal component analysis of MSBAS DInSAR time series from Campi Flegrei, Italy. Journal of Volcanology and Geothermal Research, 2017, 344, 139-153.	2.1	12
82	3D multi-source model of elastic volcanic ground deformation. Earth and Planetary Science Letters, 2020, 547, 116445.	4.4	12
83	Leveraging time series analysis of radar coherence and normalized difference vegetation index ratios to characterize pre-failure activity of the Mud Creek landslide, California. Natural Hazards and Earth System Sciences, 2021, 21, 629-642.	3.6	12
84	Threeâ€dimensional indirect boundary element method for deformation and gravity changes in volcanic areas: Application to Teide volcano (Tenerife, Canary Islands). Journal of Geophysical Research, 2007, 112, .	3.3	11
85	Some Insights into Topographic, Elastic and Self-gravitation Interaction in Modelling Ground Deformation and Gravity Changes in Active Volcanic Areas. Pure and Applied Geophysics, 2007, 164, 865-878.	1.9	11
86	Interpretation of 1992–1994 Gravity Changes around Mayon Volcano, Philippines, Using Point Sources. Pure and Applied Geophysics, 2007, 164, 733-749.	1.9	11
87	Identification of Glacial Isostatic Adjustment in Eastern Canada Using S Transform Filtering of GPS Observations. Pure and Applied Geophysics, 2012, 169, 1507-1517.	1.9	11
88	Foreshock and Aftershocks in Simple Earthquake Models. Physical Review Letters, 2015, 114, 088501.	7.8	11
89	Changing the Culture of Fieldwork in the Geosciences. Eos, 2021, 102, .	0.1	11
90	Measuring the state and temporal evolution of glaciers in Alaska and Yukon using synthetic-aperture-radar-derived (SAR-derived) 3D time series of glacier surface flow. Cryosphere, 2021, 15, 4221-4239.	3.9	11

#	Article	IF	CITATIONS
91	Forecasting rupture dimension using the pattern informatics technique. Tectonophysics, 2006, 424, 367-376.	2.2	10
92	Spatiotemporal gravity changes on volcanoes: Assessing the importance of topography. Geophysical Research Letters, 2009, 36, .	4.0	10
93	Preface for "Earthquake Hazard Evaluation― Pure and Applied Geophysics, 2013, 170, 1-2.	1.9	10
94	Scaling of earthquake models with inhomogeneous stress dissipation. Physical Review E, 2013, 87, 022809.	2.1	10
95	Shallow Hydrothermal Pressurization before the 2010 Eruption of Mount Sinabung Volcano, Indonesia, Observed by use of ALOS Satellite Radar Interferometry. Pure and Applied Geophysics, 2015, 172, 3229-3245.	1.9	10
96	A revision of the FORTRAN codes GRAVW to compute deformation produced by a point magma intrusion in elastic-gravitational layered earth models. Computers and Geosciences, 2006, 32, 275-281.	4.2	9
97	The Stress Accumulation Method and the Pattern Informatics Index: Complementary Approaches to Earthquake Forecasting. Pure and Applied Geophysics, 2008, 165, 693-709.	1.9	9
98	GEM Plate Boundary Simulations for the Plate Boundary Observatory: A Program for Understanding the Physics of Earthquakes on Complex Fault Networks via Observations, Theory and Numerical Simulation. , 2002, , 2357-2381.		9
99	Accuracy, Efficiency, and Transferability of a Deep Learning Model for Mapping Retrogressive Thaw Slumps across the Canadian Arctic. Remote Sensing, 2022, 14, 2747.	4.0	9
100	Observation of systematic variations in non-local seismicity patterns from southern California. Geophysical Monograph Series, 2000, , 211-218.	0.1	8
101	Topography and self-gravitation interaction in elastic-gravitational modeling. Geochemistry, Geophysics, Geosystems, 2007, 8, n/a-n/a.	2.5	8
102	The spatial and temporal subsidence variability of the East Mesa Geothermal Field, California, USA, and its potential impact on the All American Canal System. International Journal of Remote Sensing, 2011, 32, 3427-3449.	2.9	8
103	Optimization of Seismicity-Based Forecasts. Pure and Applied Geophysics, 2013, 170, 139-154.	1.9	8
104	Results for aseismic creep on the Hayward fault using polarization persistent scatterer InSAR. Earth and Planetary Science Letters, 2013, 367, 157-165.	4.4	8
105	Multibaseline PolInSAR Using RADARSAT-2 Quad-Pol Data: Improvements in Interferometric Phase Analysis. IEEE Geoscience and Remote Sensing Letters, 2013, 10, 1280-1284.	3.1	8
106	Integration of DInSAR Time Series and GNSS Data for Continuous Volcanic Deformation Monitoring and Eruption Early Warning Applications. Remote Sensing, 2022, 14, 784.	4.0	8
107	Stress Shadows Determined from a Phase Dynamical Measure of Historic Seismicity. Pure and Applied Geophysics, 2006, 163, 2407-2416.	1.9	7
108	Space- and Time-Dependent Probabilities for Earthquake Fault Systems from Numerical Simulations: Feasibility Study and First Results. Pure and Applied Geophysics, 2010, 167, 967-977.	1.9	7

#	Article	IF	CITATIONS
109	Effects of Location Errors in Pattern Informatics. Pure and Applied Geophysics, 2013, 170, 185-196.	1.9	7
110	Scenario shakemaps for Montreal. Canadian Journal of Civil Engineering, 2015, 42, 463-476.	1.3	7
111	Tidal Influence on Seismic Activity During the 2011–2013 El Hierro Volcanic Unrest. Tectonics, 2021, 40, e2020TC006201.	2.8	7
112	Detection of Flood Extent Using Sentinel-1A/B Synthetic Aperture Radar: An Application for Hurricane Harvey, Houston, TX. Remote Sensing, 2022, 14, 2261.	4.0	7
113	Ergodicity in Natural Fault Systems. Pure and Applied Geophysics, 2004, 161, 1957.	1.9	6
114	A gravity gradient method for characterizing the post-seismic deformation field for a finite fault. Geophysical Journal International, 2008, 173, 802-805.	2.4	6
115	Time series analysis of subsidence at Tauhara and Ohaaki geothermal fields, New Zealand, observed by ALOS PALSAR interferometry during 2007–2009. Canadian Journal of Remote Sensing, 2010, 36, S327-S334.	2.4	6
116	Towards sub-lithospheric stress determination from seismic Moho, topographic heights and GOCE data. Journal of Asian Earth Sciences, 2016, 129, 1-12.	2.3	6
117	GPS coordinate time series measurements in Ontario and Quebec, Canada. Journal of Geodesy, 2017, 91, 653-683.	3.6	6
118	Short-Term Surface Deformation on the Northern Hayward Fault, CA, and Nearby Landslides Using Polarimetric SAR Interferometry (PolInSAR). Pure and Applied Geophysics, 2015, 172, 2179-2193.	1.9	5
119	DisasterAWARE – A GLOBAL ALERTING PLATFORM FOR FLOOD EVENTS. ISPRS Annals of the Photogrammetry, Remote Sensing and Spatial Information Sciences, 0, VI-3/W1-2020, 107-113.	0.0	5
120	An Elliptical Model for Deformation Due to Groundwater Fluctuations. Pure and Applied Geophysics, 2012, 169, 1443-1456.	1.9	4
121	A correlation based stochastic partitional algorithm for accurate cluster analysis. International Journal of Signal and Imaging Systems Engineering, 2013, 6, 52.	0.6	4
122	Big Data Challenges and Hazards Modeling. , 2018, , 193-210.		4
123	Modelling the elevation-dependent seasonal amplitude of tropospheric delays in GPS time-series using DInSAR and meteorological data. Geophysical Journal International, 2019, 216, 676-691.	2.4	4
124	Describing Seismic Pattern Dynamics by Means of Ising Cellular Automata. Lecture Notes in Earth Sciences, 2008, , 273-290.	0.5	4
125	Parallelization of a large-scale computational earthquake simulation program. Concurrency Computation Practice and Experience, 2002, 14, 531-550.	2.2	3
126	Study of Volcanic Sources at Long Valley Caldera, California, Using Gravity Data and a Genetic Algorithm Inversion Technique. Pure and Applied Geophysics, 2004, 161, 1399-1413.	1.9	3

#	Article	IF	CITATIONS
127	Earthquakes: Simulations, Sources and Tsunamis. Pure and Applied Geophysics, 2008, 165, 449-450.	1.9	3
128	Postseismic Deformation Following the 1994 Northridge Earthquake Identified Using the Localized Hartley Transform Filter. Pure and Applied Geophysics, 2008, 165, 1577-1602.	1.9	3
129	Using Borehole Records to Estimate Magnitude for Earthquake and Tsunami Early-Warning Systems. Bulletin of the Seismological Society of America, 2013, 103, 2216-2226.	2.3	3
130	Spatial Heterogeneity in Earthquake Fault-Like Systems. Pure and Applied Geophysics, 2015, 172, 2167-2177.	1.9	3
131	A multiâ€sensor evaluation of precipitation uncertainty for landslideâ€triggering storm events. Hydrological Processes, 2021, 35, e14260.	2.6	3
132	Spatiotemporal Analysis of Ground Deformation at Campi Flegrei and Mt Vesuvius, Italy, Observed by Envisat and Radarsat-2 InSAR During 2003–2013. Lecture Notes in Earth System Sciences, 2014, , 377-382.	0.6	3
133	Methods for Evaluation of Geodetic Data and Seismicity Developed with Numerical Simulations: Review and Applications. Pure and Applied Geophysics, 2004, 161, 1489-1507.	1.9	2
134	Deformations occurring in the city of Auckland, New Zealand as mapped by the differential synthetic aperture radar. , 2008, , .		2
135	DInSAR, CPS and gravity observation results in La Palma, Canary islands. , 2008, , .		2
136	MODELS OF EARTHQUAKE FAULTS: ERGODICITY AND FORECASTING. International Journal of Modern Physics B, 2009, 23, 5553-5569.	2.0	2
137	Largeâ€scale numerical simulations of earthquake fault systems: illuminating the role of dilatational gravity in earthquake nucleation. Concurrency Computation Practice and Experience, 2010, 22, 1644-1652.	2.2	2
138	Inverting for source parameters using a genetic algorithm applied to deformation signals observed at the Auckland Volcanic Field. Canadian Journal of Remote Sensing, 2010, 36, S266-S273.	2.4	2
139	Characterizing Large Events and Scaling in Earthquake Models With Inhomogeneous Damage. Geophysical Monograph Series, 2012, , 41-54.	0.1	2
140	Anomalous statistics of aftershock sequences generated by supershear ruptures. Research in Geophysics, 2012, 2, 6.	0.7	2
141	A Pipelining Implementation for High Resolution Seismic Hazard Maps Production. Procedia Computer Science, 2015, 51, 1473-1482.	2.0	2
142	Improved Real-Time Natural Hazard Monitoring Using Automated DInSAR Time Series. Remote Sensing, 2021, 13, 867.	4.0	2
143	[Comment on "Exaggerated claims about earthquake predictions: Analysis of NASA's methodâ€] Pattern informatics and cellular seismology: A comparison of methods. Eos, 2007, 88, 254-254.	0.1	1
144	A Hybrid Model for the Summit Region of Merapi Volcano, Java, Indonesia, Derived from Gravity Changes and Deformation Measured between 2000 and 2002. Pure and Applied Geophysics, 2007, 164, 837-850.	1.9	1

#	Article	IF	CITATIONS
145	Surface deformation studies of Tenerife Island, Spain from joint GPS-DInSAR observations. , 2008, , .		1
146	Enhancement of the frequency resolution of the S-transform using the fourier transform. , 2011, , .		1
147	Probability Gain From Seismicity-Based Earthquake Models. , 2018, , 175-192.		1
148	Space- and Time-Dependent Probabilities for Earthquake Fault Systems from Numerical Simulations: Feasibility Study and First Results. , 2010, , 113-123.		1
149	Pattern Dynamics and Forecast Methods in Seismically Active Regions. , 2002, , 2429-2467.		1
150	Statistical Mechanics Perspective on Earthquakes. Understanding Complex Systems, 2017, , 1-18.	0.6	1
151	Real-Time Earthquake Intensity Estimation Using Streaming Data Analysis of Social and Physical Sensors. Pageoph Topical Volumes, 2018, , 137-155.	0.2	1
152	Insights into seismic hazard from big data analysis of ground motion simulations. International Journal of Safety and Security Engineering, 2019, 9, 01-12.	1.0	1
153	Characterization of large tsunamigenic landslides and their effects using digital surface models: A case study from Taan Fiord, Alaska. Remote Sensing of Environment, 2022, 270, 112881.	11.0	1
154	Correction to "Critical point theory of earthquakes: Observation of correlated and cooperative behavior on earthquake fault systemsâ€. Geophysical Research Letters, 2007, 34, .	4.0	0
155	Modeling of Stress Changes at Mayon Volcano, Philippines. Pure and Applied Geophysics, 2007, 164, 819-835.	1.9	Ο
156	A general method for calculating co-seismic gravity changes in complex fault systems. Computers and Geosciences, 2008, 34, 1541-1549.	4.2	0
157	The effect of scattering processes on high frequency ground penetrating radar surveys on impact melt breccia - Early results from an arctic field campaign at the Haughton impact structure, Devon Island, Canada. , 2011, , .		0
158	Determinación geodésica del deslizamiento de falla para el terremoto de Lorca del 11 de Mayo de 2011 usando interferometrÃa radar y GPS. FÃsica De La Tierra, 2013, 24, .	0.1	0
159	Magnitude Estimation for the 2011 Tohoku-Oki Earthquake Based on Ground Motion Prediction Equations. Pure and Applied Geophysics, 2015, 172, 2139-2155.	1.9	0
160	Monitoring of urban subsidence in coastal cities: Case studies Vancouver and Seattle. , 2016, , .		0
161	Thank You to Our 2019 Reviewers. Earth and Space Science, 2020, 7, e2020EA001195.	2.6	0
162	Thank You to Our 2020 Reviewers. Earth and Space Science, 2021, 8, e2021EA001735.	2.6	0

#	Article	IF	CITATIONS
163	Stress Shadows Determined from a Phase Dynamical Measure of Historic Seismicity. , 2006, , 2407-2416.		о
164	Systematic Procedural and Sensitivity Analysis of the Pattern Informatics Method for Forecasting Large (M > 5) Earthquake Events in Southern California. , 2006, , 2433-2454.		0
165	The Stress Accumulation Method and the Pattern Informatics Index: Complementary Approaches to Earthquake Forecasting. , 2008, , 693-709.		Ο
166	Diffusion Entropy Analysis in Seismicity. , 2007, , 419-427.		0
167	Thank You to Our 2021 Reviewers. Earth and Space Science, 2022, 9, .	2.6	Ο
168	Earthquakes: Simulations, Sources and Tsunamis. , 0, , 449-450.		0